

Percolation *via* combined electrostatic and chemical doping in complex oxide films

Peter P. Orth,¹ Rafael M. Fernandes,¹ Jeff Walter,² C. Leighton,² and B. I. Shklovskii^{1,3}

¹*School of Physics and Astronomy, University of Minnesota, Minneapolis, Minnesota 55455, USA*

²*Department of Chemical Engineering and Materials Science,
University of Minnesota, Minneapolis, MN 55455, USA*

³*Fine Theoretical Physics Institute, University of Minnesota, Minneapolis, MN 55455, USA*

(Dated: November 27, 2021)

Stimulated by experimental advances in electrolyte gating methods, we investigate theoretically percolation in thin films of inhomogeneous complex oxides, such as $\text{La}_{1-x}\text{Sr}_x\text{CoO}_3$ (LSCO), induced by a combination of bulk chemical and surface electrostatic doping. Using numerical and analytical methods, we identify two mechanisms that describe how bulk dopants reduce the amount of electrostatic surface charge required to reach percolation: (i) bulk-assisted surface percolation, and (ii) surface-assisted bulk percolation. We show that the critical surface charge strongly depends on the film thickness when the film is close to the chemical percolation threshold. In particular, thin films can be driven across the percolation transition by modest surface charge densities *via* surface-assisted bulk percolation. If percolation is associated with the onset of ferromagnetism, as in LSCO, we further demonstrate that the presence of critical magnetic clusters extending from the film surface into the bulk results in considerable volume enhancement of the saturation magnetization, with pronounced experimental consequences. These results should significantly guide experimental work seeking to verify gate-induced percolation transitions in such materials.

Introduction.—The rapidly growing field of complex oxide heterostructures provides many opportunities for the observation of new physical phenomena, with promising applications in future electronic devices [1–3]. Examples include strain engineering to control structural and electronic ground states [1–4], realization of novel two-dimensional (2D) electron gases at oxide interfaces [3, 5, 6], and the observation of interfacial magnetic [1–3, 7] and superconducting states [1–3]. Due to the lower charge carrier densities in these materials ($n \simeq 10^{21}\text{cm}^{-3}$) compared to conventional metals ($n \simeq 10^{23}\text{cm}^{-3}$), surface electrostatic or electrochemical control of these novel properties *via* the electric field effect also becomes an exciting possibility [2, 8–10].

Stimulated by the above situation, high- κ dielectrics, ferroelectric gating, and electrolyte gating (primarily with ionic liquids and gels) have been successfully employed to electrostatically induce and control large charge densities in these materials [2, 8–10]. Particularly prominent recent progress has been made with ionic liquid and gel gating, the surface carrier densities achieved routinely exceeding $s \simeq 10^{14}\text{cm}^{-2}$, corresponding to modulation of significant fractions of an electron (or hole) per unit cell [2, 8–10]. This has, for example, enabled reversible external electrical control of oxide electronic phase transitions from insulating to metallic [11–14], to a superconducting state [15–17], or from paramagnetic to magnetically-ordered phases [18, 19]. Nevertheless, attainment of sufficient charge density to induce the phase transitions of interest remains a challenge in many cases, due to the need for $s \simeq 10^{15}\text{cm}^{-2}$. In such cases one obvious strategy is to employ a combination of chemical and electrostatic doping, bringing the material close to some electronic/magnetic phase boundary by chemical substitution, then using surface electrostatic tuning

of the carrier density to reversibly traverse the critical point.

The work presented here focuses on exactly such combined electrostatic surface and bulk chemical doping. In particular, we investigate electronic/magnetic percolation transitions induced by a combination of chemical

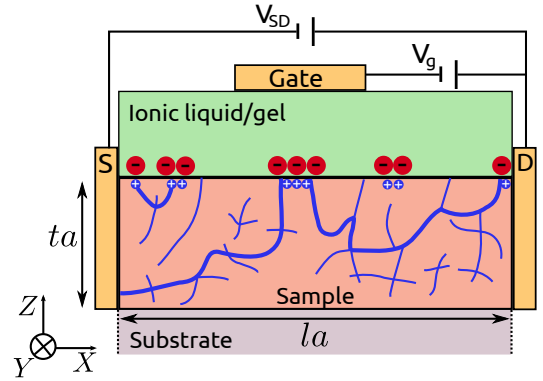


FIG. 1. Schematic setup showing a thin film sample (red) of thickness ta and area $la \times la$, where a is the lattice constant, with large finite clusters (blue) due to bulk doping. The ionic liquid or gel (light green) on top of the sample induces a number of holes (blue spheres) at the top surface – proportional to the applied gate voltage V_g . Red spheres denote anions in the ionic liquid/gel that move towards the surface due to the applied voltage. For bulk doping close to percolation $x_c - x \ll 1$ (surface-assisted bulk percolation), electrostatically induced holes connect finite bulk clusters at the surface resulting in a conducting path (highlighted in the figure) between source (S) and drain (D) electrodes. This leads to a current driven by an applied source-drain voltage V_{SD} . The highlighted upper left cluster shows bulk bridges connecting two surface clusters, which is the dominant effect of bulk dopants for $x \ll x_c$ (bulk-assisted surface percolation).

and electrostatic doping. This is an important situation in complex oxide materials due to the widespread observation of electronic and magnetic inhomogeneity (as in manganites [20], cuprates [21], and cobaltites [22, 23] for example), where many transitions, such as from insulator to metal or from short- to long-range magnetism, are percolative in nature. While our analysis and results are general, and could apply to percolation transitions in various materials, in this paper we are motivated by physics of the perovskite oxide cobaltite, $\text{La}_{1-x}\text{Sr}_x\text{CoO}_3$ (LSCO), which is well established to undergo a percolation transition from insulator to metal at $x_c \simeq 0.18$ [22–24].

In the parent compound LaCoO_3 ($x = 0$), the Co^{3+} ($3d^6$) ions adopt the $S = 0$ spin state as $T \rightarrow 0$, and the material is a diamagnetic semiconductor. Substituting Sr^{2+} for La^{3+} induces holes, changing the formal valence state of a neighboring Co ion to $4+$, which is in a $S > 0$ spin-state. The subsequent evolution from insulator to metal (due to hole transfer between nearest-neighbor Co^{4+}) and short- to long-range ferromagnetic correlations is caused by percolation of nanoscopic ferromagnetic hole-rich clusters [22–24]. Very thin (few unit cell thick) films of LSCO are the natural target for field-effect gating experiments, as significant modulation of the charge carrier density is confined to a narrow layer close to the surface. The layer width is of the order of the electrostatic screening length, which is typically one or two unit cells [2, 8–10] due to the large carrier densities ($n \simeq 10^{21}\text{cm}^{-3}$) in significantly doped LSCO.

The theoretical study of percolation phenomena in correlated systems has a long history [25–33]. However, the combination of bulk chemical and surface electrostatic doping defines an interesting and unusual percolation problem that is so far largely unexplored theoretically. The schematic setup with gate, source and drain electrodes is shown in Fig. 1, where the blue parts in the LSCO film denote hole-rich regions and the top surface is affected by electrostatic gating. The total (top) surface carrier density,

$$s = x + \Delta s \quad (1)$$

arises from doping both by chemical substitution of a fraction of lattice sites x and electrostatic gating of a fraction of surface lattice sites Δs .

In this work we identify two different percolation phenomena: bulk-assisted surface percolation and surface-assisted bulk percolation, which are schematically depicted in Fig. 1. In the first case, where the system is initially far away from the (thickness-dependent) bulk percolation threshold $x_c(t)$, percolation on the surface is facilitated by diluted bulk dopants, which provide bridges that connect disjunct finite surface clusters. As a result, the amount of surface charge Δs_c that must be induced electrostatically to reach percolation is insensitive to the

film thickness. In the second case, where the bulk chemical doping level is close to the percolation threshold, $x_c(t) - x \ll 1$, we find that small Δs helps to reach bulk percolation by connecting large finite bulk clusters on the surface. We show that the surface charge at percolation follows $s_c \propto t(x_c - x)$ for films of thickness ta . As a result, Δs_c grows moderately with $(x_c - x)$ for thin films, but increases sharply for thicker films. In the particular case where the percolation transition is associated with ferromagnetic order, as in LSCO, the presence of clusters, which extend from the surface into the bulk, greatly enhance the surface saturation magnetization M_s .

Numerical modeling of percolation.— To derive our results, we consider the site percolation problem on the cubic lattice of size $la \times la \times ta$ along the X , Y and Z axes defined in Fig. 1, where a is the lattice constant and l, t are integers ($t \leq l$). This geometry describes films of thickness ta and surface area $(la)^2$. The percolation problem is solved using the numerical algorithm described in Refs. 34 and 35. Starting from an empty lattice, a fraction x of sites are first randomly filled in the whole lattice to simulate bulk chemical doping. We verify that the bulk doping percolation threshold on the isotropic cubic lattice ($l = t$) lies at $x_c^{3D} = 0.31$ [36], and increases for $t < l$, i.e., $x_c(t) > x_c(l) \equiv x_c^{3D}$ [25]. To study the role of surface doping, we stop at a bulk doping level $x < x_c(t)$ and subsequently add a fraction Δs of sites exclusively on the top surface layer to simulate electrostatic gating. The total surface density of sites at the top surface is then given by Eq. (1). While electrostatically doping the system, we continuously monitor whether a percolating path exists between the two side surfaces at $X = 0$ and $X = la$. We define the critical total density of sites at the top surface that is required for percolation between the side surfaces as s_c . The amount of charge density that must be transferred *via* electrostatic doping is then denoted Δs_c .

In Fig. 2(a), we show numerical results for Δs_c as a function of the starting bulk chemical doping level x ; panel (b) shows s_c as a function of x . For pure surface doping, $x = 0$, we find the percolation threshold of the 2D square lattice, $\Delta s_c(0) = 0.59$ [26]. For small $x \ll x_c(t)$, the behavior of $\Delta s_c(x)$ depends only weakly on the film thickness t . In contrast, for $x_c(t) - x \ll 1$ the function $\Delta s_c(x)$ depends strongly on the thickness t , displaying a sharp enhancement as x decreases for thick films but a much more gradual one for thin films. To understand the numerical results, we next employ scaling theory arguments [25].

Analytical theory.— To develop an analytical theory, we focus on three limits: (i) $x \ll x_c(t)$, (ii) $x_c^{3D} - x \ll 1$ and (iii) $x_c(t) - x \ll 1$, which are indicated by yellow rectangles in Fig. 2(a). The first case can be described as bulk-assisted surface percolation and the other two by surface-assisted bulk percolation.

(i) For $x \ll x_c(t)$, we have $s_c(0) - s_c(x) \ll 1$: the sys-

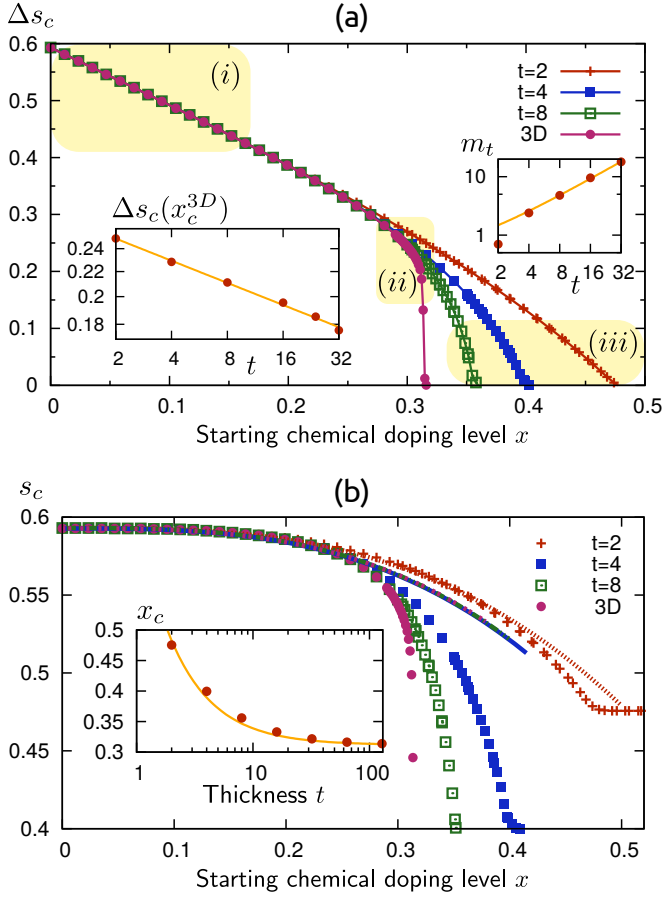


FIG. 2. (a) Surface charge density Δs_c that must be electrostatically induced to reach percolation, as a function of starting bulk chemical doping level, x . Different curves correspond to different thicknesses t , as indicated, and are obtained from extrapolating results for system sizes $l \times l \times t$ with $l = 32, 64, 128$ to $l^{-1} \rightarrow 0$ and are averaged over at least 4.1×10^5 disorder realizations. The curve labelled “3D” is for $t = l$. The left inset shows that Δs_c at the bulk percolation threshold $x_c^{3D} = 0.31$ obeys Eq. (4) (yellow line) with $c_2 = 0.27$. The right inset shows the slope of $s_c - x_c = m_t(x_c - x)$ close to $x_c(t) - x \ll 1$ verifying Eq. (6) with $c_5 = 0.56$. Yellow rectangles mark the three regimes labelled (i), (ii), and (iii), addressed by our analytical theory. (b) Total surface charge at percolation, s_c , as a function of x . The lines are fits of the numerical results according to Eq. (2) with $b = 0.91$ for $t = 2$ and $b = 1.12$ for $t = 4, 8, l$. The inset shows the thickness-dependent bulk percolation threshold $x_c(t)$ for purely chemical doping. The yellow line obeys Eq. (5) with $x_c^{3D} = 0.312$, $\nu = 0.88$ [36] and $c_3 = 1.21$.

tem is close to the 2D percolation threshold on the surface, but far from percolation in the bulk. As a result, the typical size of bulk clusters is rather small. These small bulk clusters can still assist percolation at the surface by providing short bridges across missing links between disconnected finite large surface clusters. This situation is shown schematically in Fig. 1. Since the smallest possible bulk bridge consists of three sites below the surface,

at $x \ll 1$ the main contribution of the bulk doping arises from such bridges, yielding

$$s_c(x) = s_c(0) - bx^3. \quad (2)$$

As shown in Fig. 2(b), this equation, with weakly t -dependent coefficient b , describes the numerical results well for $s_c(0) - s_c(x) \ll 1$; for $t = 2$ it is even applicable over almost the full range of doping levels up to x_c .

(ii) In the regime of small $x_c^{3D} - x \ll 1$, the 3D bulk is close to the percolation threshold, but the surface concentration is far from the surface percolation threshold. Thus, while large critical finite clusters exist in the bulk, with a typical size of $\xi(x) \sim a(x_c^{3D} - x)^{-\nu}$ and correlation length exponent $\nu = 0.88$ [26, 36], the largest surface clusters remain small.

Let us first discuss the case of an infinite isotropic 3D system, before considering finite thickness films. If sites were randomly added in the bulk, an infinite cluster connecting $X = 0$ and $X = la$, which looks like a network of links and nodes with typical separation $\xi(x)$, would occur after adding $N = N_0(x_c^{3D} - x)l^3$ sites, with $N_0 \simeq 2$. Because this infinite cluster provides percolation inside a layer of height $\xi(x)$ below the surface, the number of sites $\Delta N = N_0(x_c^{3D} - x)l^2\xi(x)/a$ we have added to this layer is sufficient to induce percolation along the layer. It is now plausible that instead of homogeneously doping the sliver of volume $(la)^2\xi(x)$, we can reach percolation by adding all these sites to the surface plane only. For a 3D system, this yields a critical surface density of

$$s_c(x) = x_c^{3D} + \frac{\Delta N}{l^2} = x_c^{3D} + c_1(x_c^{3D} - x)^{1-\nu}, \quad (3)$$

with a non-universal constant c_1 and $x_c^{3D} - x \ll 1$. We see that since $\nu < 1$, connecting bulk clusters on the surface can be done by very small surface addition Δs at $x_c^{3D} - x \ll 1$. Of course, the scaling behavior in Eq. (3) only holds as long as $(x_c^{3D} - x)^{1-\nu} \ll 1$. Since $1 - \nu = 0.12 \ll 1$ [26, 36], the validity of Eq. (3) is therefore limited to a tiny region of x close to x_c . This explains the sharp enhancement of $\Delta s_c(x)$ observed in the 3D numerical results shown in Fig. 2.

A finite thickness t of the film introduces another length scale, which cuts off the scaling behavior of Eq. (3) as soon as the correlation length becomes larger than the film thickness. We will now show that for bulk doping levels such that $\xi(x) \geq ta$, Eq. (3) is replaced by

$$s_c(x) = x_c^{3D} + c_2 t^{1-1/\nu}, \quad (4)$$

with non-universal constant c_2 . We numerically verify this scaling behavior at $x = x_c^{3D}$ as shown in the (left) inset of Fig. 2(a). To derive Eq. (4), we first notice that the bulk percolation threshold $x_c(t)$ of a film of thickness t is reached when an infinite bulk cluster with correlation length $\xi[x_c(t)] \leq ta$ appears. From this it follows

that [25]:

$$x_c(t) = x_c^{3D} + c_3 t^{-1/\nu}, \quad (5)$$

with non-universal constant $c_3 = 1.21$, which is in agreement with our numerical results shown in the inset of Fig. 2(b). Therefore, to achieve percolation at $x \simeq x_c^{3D}$, a film with width t must acquire $\Delta N = c_4(x_c(t) - x_c^{3D})t l^2 = c_2 l^2 t^{1-1/\nu}$ filled sites, where c_4 is a non-universal constant. As above, we assume that we can reach the percolation threshold by bringing all these sites into the surface plane by electrostatic gating, yielding Eq. (4). Note that Eq. (4) crosses over to Eq. (3) at $\xi(x) = ta$.

(iii) We now investigate s_c for $x_c(t) - x \ll 1$. In this regime, it holds that $\xi(x) > ta$ since the correlation length at $x_c(t)$ fulfills $\xi[x_c(t)] = ta$. In this case, we find that $\Delta N = (x_c(t) - x)l^2 t$ sites should be added to the system in order to reach percolation, such that the critical surface percolation threshold obeys

$$s_c(x) = x_c(t) + c_5 t(x_c(t) - x) \quad (6)$$

with non-universal constant c_5 . We demonstrate in the (right) inset of Fig. 2(a) that our numerical results follow this scaling relation of the slope $m_t = c_5 t$ with $c_5 = 0.56$. Note that the scaling breaks down for the thinnest system, $t = 2$, which is instead described by Eq. (2) over the full range of bulk doping levels x (see Fig. 2(b)).

The key insight from the combined numerical and analytical results is that bulk chemical doping largely reduces the amount of electrostatic surface charge Δs_c required to reach percolation (compared to the 2D value) in a region of initial chemical doping levels $x_c^{3D} < x < x_c(t)$. In this regime, the critical surface charge s_c scales with the thickness according to Eq. (6) and therefore grows quickly for thicker films. The underlying physical phenomenon is that less surface charge must be transferred by electrostatic gating if percolation is induced by connecting finite large bulk clusters on the surface rather than creating a percolating path that is confined to the surface alone. The width of this region $x_c - x_c^{3D} \propto t^{-1/\nu}$ rapidly narrows for thicker films. For smaller x the dominant effect of the bulk dopants is to act as short bridges between disconnected surface clusters. This reduces the number of surface sites that must be filled to reach percolation only slightly compared to the 2D case, as described by Eq. (2).

Enhanced surface magnetization.— If the percolation transition is associated with ferromagnetic ordering, as for LSCO, the extension of the percolating cluster from the surface into the bulk leads to a dramatic volume enhancement of the surface saturation magnetization M_s in the case of surface-assisted bulk percolation (cases (ii) and (iii)). To capture this phenomenon, in Fig. 3 we show the size (*i.e.* number of sites), of the largest cluster N_c (per surface area l^2) as a function of electrostatic doping Δs . Beyond the percolation threshold $\Delta s > \Delta s_c(x)$

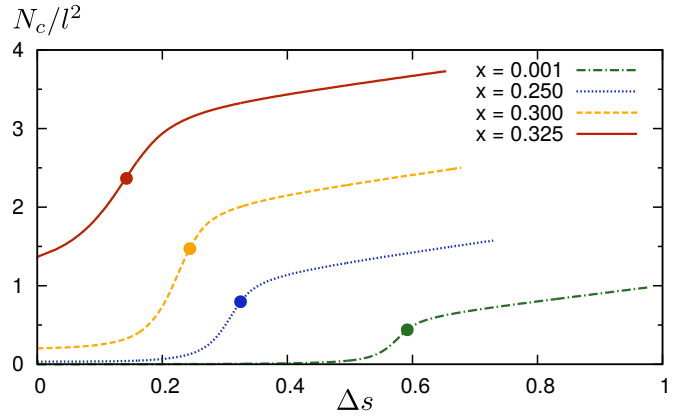


FIG. 3. Surface density of the largest cluster in the system, N_c/l^2 , as a function of electrostatic doping Δs in a film of thickness $t = 16$. Dots indicate percolation thresholds. After crossing the percolation threshold the largest cluster density is proportional to the surface saturation magnetization M_s . The plot shows the large (volume) enhancement of M_s , which occurs due to extension of the infinite cluster and its dead ends deep into the bulk (see Fig. 1).

this cluster percolates and its size is proportional to the surface saturation magnetization $M_s \propto N_c/l^2$. Different curves correspond to different starting chemical doping levels $0.003 \leq x/x_c(t) \leq 0.976$ and the film thickness is $t = 16$.

For small doping levels, we observe regular surface percolation at $\Delta s_c = 0.59$ (the percolation threshold is indicated by the dot). The percolated path is almost entirely confined to the top surface layer and the magnetization enhancement is absent: $N_c/l^2 \lesssim 1$. On the other hand, if the system is initially doped closer to the (bulk) percolation threshold x_c , the percolating cluster extends significantly into the bulk and we observe $N_c/l^2 > 1$ for the other three realistic doping levels x we consider. As the (fractal) dimension of this cluster exceeds $d = 2$, we find that N_c/l^2 becomes as large as 4 for a film of thickness $t = 16$ (note that a fully magnetized film corresponds to $N_c/l^2 = t$). This shows that although bulk doping does not assist greatly in *reaching* percolation, it does ultimately generate a much larger saturation magnetization in the sample, because of the inclusion of preformed clusters of spin polarized sites (see also Fig. 1). In addition, we further predict an unusual depth profile of magnetization $M_s(z)$ as a function of distance z from the surface, which can be directly experimentally measured, for instance using polarized neutron reflectometry. It could also be indirectly inferred using perhaps x-ray magnetic circular dichroism (XMCD) or the magneto-optical Kerr effect (MOKE).

Conclusions.— Motivated by existing and ongoing experiments on complex oxide thin films, we have studied a new percolation problem, where bulk chemical doping is combined with electrostatic doping of the surface. We

have derived new analytical formulae describing universal scaling behavior of the electrostatic percolation threshold and explored the full crossover from bulk to surface percolation numerically. Experimental predictions that follow from our analysis are that: (i) the critical surface charge density at percolation s_c depends only weakly on the starting bulk doping level x , except in proximity to the bulk percolation transition $x_c^{3D} < x < x_c(t)$. The crossover from surface-assisted to bulk-assisted percolation occurs more abruptly for thicker films. Given limitations of ionic liquid/gel or ferroelectric gating, experimental validations of gate-induced percolation may thus rely in most cases on chemically doping close to the percolation threshold. (ii) Once percolation is reached, the saturation magnetization M_s is largely enhanced due to the presence of critical clusters extending deep into the bulk. (iii) The existence of ferromagnetic bulk clusters will also be reflected in the dependence of the magnetization $M_s(z)$ on the distance z from the surface. Our work thus shows that “bulk” magnetic properties can be controlled using “surface” electrostatic gating. We note that while the percolation threshold x_c is a non-universal quantity dependent on microscopic details such as the geometry of the lattice, the scaling behavior of $s_c(x)$ that we derive is *universal*. Our results thus apply to LSCO and other experimental systems even though the percolation threshold in this material is not that of a simple cubic lattice $x_c^{3D} \simeq 0.31$, but rather $x_{c,LSCO}^{3D} \simeq 0.18$. Finally, we note that while our analysis has focused on effects of electrostatic gating, our conclusions also apply to the case of electrochemical doping describing, for example, the transfer of oxygen vacancies into the surface of a sample.

We gratefully acknowledge useful discussions with K. Reich. This work was supported primarily by the National Science Foundation through the University of Minnesota MRSEC under Award Number DMR-1420013. We acknowledge the Minnesota Supercomputing Institute (MSI) at the University of Minnesota for providing resources that contributed to the research results of this work.

-
- [1] P. Zubko, S. Gariglio, M. Gabay, P. Ghosez, and J.-M. Triscone, *Annu. Rev. Cond. Mat. Phys.* **2**, 141 (2011).
 - [2] J. Ngai, F. Walker, and C. Ahn, *Annu. Rev. Mater. Res.* **44**, 1 (2014).
 - [3] J. A. Sulpizio, S. Ilani, P. Irvin, and J. Levy, *Annu. Rev. Mater. Res.* **44**, 117 (2014).
 - [4] J. H. Haeni, P. Irvin, W. Chang, R. Uecker, P. Reiche, Y. L. Li, S. Choudhury, W. Tian, M. E. Hawley, B. Craigo, A. K. Tagantsev, X. Q. Pan, S. K. Streiffer, L. Q. Chen, S. W. Kirchoefer, J. Levy, and D. G. Schlom, *Nature* **430**, 758 (2004).
 - [5] A. Ohtomo and H. Hwang, *Nature* **427**, 423 (2004).
 - [6] S. Stemmer and S. J. Allen, *Annu. Rev. Mater. Res.* **44**, 151 (2014).
 - [7] A. Bhattacharya and S. J. May, *Annu. Rev. Mater. Res.* **44**, 65 (2014).
 - [8] C. H. Ahn, A. Bhattacharya, M. Di Ventra, J. N. Eckstein, C. D. Frisbie, M. E. Gershenson, A. M. Goldman, I. H. Inoue, J. Mannhart, A. J. Millis, A. F. Morpurgo, D. Natelson, and J.-M. Triscone, *Rev. Mod. Phys.* **78**, 1185 (2006).
 - [9] C. H. Ahn, J.-M. Triscone, and J. Mannhart, *Nature (London)* **424**, 1015 (2003).
 - [10] A. M. Goldman, *Annu. Rev. Mater. Res.* **44**, 45 (2014).
 - [11] S. Asanuma, P.-H. Xiang, H. Yamada, H. Sato, I. H. Inoue, H. Akoh, A. Sawa, K. Ueno, H. Shimotani, H. Yuan, M. Kawasaki, and Y. Iwasa, *Appl. Phys. Lett.* **97**, 142110 (2010).
 - [12] R. Scherwitzl, P. Zubko, I. G. Lezama, S. Ono, A. F. Morpurgo, G. Catalan, and J.-M. Triscone, *Adv. Mater.* **22**, 5517 (2010).
 - [13] M. Nakano, K. Shibuya, D. Okuyama, T. Hatano, S. Ono, M. Kawasaki, Y. Iwasa, and Y. Tokura, *Nature* **487**, 459 (2012).
 - [14] J. Jeong, N. Aetukuri, T. Graf, T. D. Schladt, M. G. Samant, and S. S. P. Parkin, *Science* **339**, 1402 (2013).
 - [15] K. Ueno, S. Nakamura, H. Shimotani, A. Ohtomo, N. Kimura, T. Nojima, H. Aoki, Y. Iwasa, and M. Kawasaki, *Nat. Mat.* **7**, 855 (2008).
 - [16] A. T. Bollinger, G. Dubuis, J. Yoon, D. Pavuna, J. Misewich, and I. Bozovic, *Nature* **472**, 458 (2011).
 - [17] X. Leng, J. Garcia-Barriocanal, S. Bose, Y. Lee, and A. M. Goldman, *Phys. Rev. Lett.* **107**, 027001 (2011).
 - [18] H. J. A. Molegraaf, J. Hoffman, C. A. F. Vaz, S. Gariglio, D. van der Marel, C. H. Ahn, and J.-M. Triscone, *Adv. Mater.* **21**, 3470 (2009).
 - [19] Y. Yamada, K. Ueno, T. Fukumura, H. T. Yuan, H. Shimotani, Y. Iwasa, L. Gu, S. Tsukimoto, Y. Ikuhara, and M. Kawasaki, *Science* **332**, 1065 (2011).
 - [20] E. Dagotto, T. Hotta, and A. Moreo, *Phys. Rep.* **344**, 1 (2001).
 - [21] A. N. Pasupathy, A. Pushp, K. K. Gomes, C. V. Parker, J. Wen, Z. Xu, G. Gu, S. Ono, Y. Ando, and A. Yazdani, *Science* **320**, 196 (2008).
 - [22] J. Wu and C. Leighton, *Phys. Rev. B* **67**, 174408 (2003).
 - [23] C. He, S. El-Khatib, J. Wu, J. W. Lynn, H. Zheng, J. F. Mitchell, and C. Leighton, *EPL* **87**, 27006 (2009).
 - [24] C. He, S. El-Khatib, S. Eisenberg, M. Manno, J. W. Lynn, H. Zheng, J. F. Mitchell, and C. Leighton, *Appl. Phys. Lett.* **95**, 222511 (2009).
 - [25] B. I. Shklovskii and A. L. Efros, *Electronic Properties of Doped Semiconductors*, Springer Series in Solid-State Sciences, Vol. 45 (Springer, Heidelberg, 1984).
 - [26] D. Stauffer and A. Aharony, *Introduction to Percolation Theory*, 2nd ed. (Taylor & Francis, London (UK), 1994).
 - [27] T. Vojta and J. Schmalian, *Phys. Rev. Lett.* **95**, 237206 (2005).
 - [28] R. Yu, T. Roscilde, and S. Haas, *Phys. Rev. Lett.* **94**, 197204 (2005).
 - [29] N. Bray-Ali, J. E. Moore, T. Senthil, and A. Vishwanath, *Phys. Rev. B* **73**, 064417 (2006).
 - [30] L. Wang and A. W. Sandvik, *Phys. Rev. Lett.* **97**, 117204 (2006).
 - [31] J. A. Hoyos, C. Kotabage, and T. Vojta, *Phys. Rev. Lett.* **99**, 230601 (2007).
 - [32] E. Altman, Y. Kafri, A. Polkovnikov, and G. Refael, *Phys. Rev. Lett.* **100**, 170402 (2008).

- [33] R. M. Fernandes and J. Schmalian, [Phys. Rev. Lett. **106**, 067004 \(2011\)](#).
- [34] M. E. J. Newman and R. M. Ziff, [Phys. Rev. Lett. **85**, 4104 \(2000\)](#).
- [35] M. E. J. Newman and R. M. Ziff, [Phys. Rev. E **64**, 016706 \(2001\)](#).
- [36] J. Wang, Z. Zhou, W. Zhang, T. M. Garoni, and Y. Deng, [Phys. Rev. E **87**, 052107 \(2013\)](#).